ORIGINAL ARTICLE

Thermodynamic investigation of SNG production based on dual fluidized bed gasification of biogenic residues

Alexander Bartik[1] · Florian Benedikt[1] · Andreas Lunzer[2] · Constantin Walcher[2] · Stefan Müller[1,2] · Hermann Hofbauer[1]

Abstract
Natural gas is an important commodity in the European energy market. The gasification of biogenic residues and the further reaction to a methane-rich gas represent a promising concept for the production of synthetic natural gas on a fossil-free basis. This paper investigates the thermodynamics of methanation in a fluidized bed reactor for different product gas compositions of the dual fluidized bed gasification technology. The investigated product gases range from conventional steam gasification, over CO_2 gasification, to product gases from the sorption enhanced reforming process. All investigated product gases from conventional steam gasification show an understoichiometric composition and therefore require a proper handling of carbon depositions and a CO_2 separation unit downstream of the methanation reactor. The product gas from CO_2 gasification is considered disadvantageous for the investigated process, because it only exhibits a carbon utilization efficiency of 23%. Due to the high flexibility of the sorption enhanced reforming process, a nearly complete methanation of the carbonaceous species is possible without the need for a CO_2 separation step or the addition of steam upstream of the methanation reactor. Furthermore, the carbon utilization efficiency is found to be between 36 and 38%, similar to the results for conventional steam gasification. Temperature and pressure variations allow a thermodynamically optimized operation, which can increase the performance of the methanation and lower the extent of gas upgrading for grid feed-in. Additionally, if a higher hydrogen content in the natural gas grid would be allowed, the overall process chain could be further optimized and simplified.

Keywords Thermodynamics · Fluidized bed methanation · Synthetic natural gas · Dual fluidized bed gasification · Biogenic residues

1 Introduction

Increasing greenhouse gas emissions and the limited availability of primary energy carriers directed the energy policy of the European Union towards sustainable and innovative energy technologies [1]. Natural gas is one of the most important primary energy carriers in Europe, but its availability is heavily dependent on the non-European market. The production of synthetic natural gas (SNG) from biogenic residues offers a promising alternative to the utilization of fossil fuels and

represents a novel concept to support the current energy strategy of the European Union [1, 2].

One possible process route is the dual fluidized bed (DFB) gasification, which allows the utilization of locally available residual biogenic or waste resources and offers possibilities for the production of highly valuable secondary energy carriers on a fossil-free basis. Wilk [3] and Benedikt et al. [4], for example, increased the fuel flexibility of the DFB process towards residues and waste for two generations of a 100 kW$_{th}$ DFB gasifier at TU Wien, while Schweitzer [5] and Schmid et al. [6, 7] further extended the feedstock towards sewage sludge and manure. In addition, the combination of the DFB technology with sorption enhanced reforming (SER) enables the production of a nitrogen-free product gas with adjustable hydrogen to carbon monoxide or hydrogen to carbon dioxide contents [8]. Before the product gas from the DFB gasification process can be fed to the methanation unit, rigorous gas cleaning is required in order to protect the

✉ Alexander Bartik
    alexander.bartik@tuwien.ac.at

[1] Institute of Chemical, Environmental and Bioscience Engineering, TU Wien, Getreidemarkt 9/166, 1060 Vienna, Austria

[2] Energy & Chemical Engineering GmbH, Waidhausenstraße 27/1/22, 1140 Vienna, Austria

🙋 Springer

downstream equipment and the methanation catalyst. Dust, tar, as well as sulfur and nitrogen containing compounds need to be removed. Gas cleaning is not further elaborated here, but in [9] a comprehensive overview over different gas cleaning strategies is provided. The exothermic methanation itself has been carried out in adiabatic or cooled fixed bed reactors, fluidized bed reactors, three-phase reactors, and structured reactors. The only commercially available reactor types thereof are adiabatic fixed bed reactors [10]. For this reactor type, many similar process concepts were developed mainly between the 1960s and the 1980s. All concepts consist of 2–7 adiabatic reactors with or without intermediate gas cooling and/or gas recycling. Two prominent representatives thereof are the TREMP and HICOM processes. Both utilize three adiabatic reactors with intermediate cooling and gas recycling. They are applied in various coal-to-SNG projects in China, whereas an adapted TREMP process is also installed in the biomass-to-SNG project GoBiGas in Sweden [11]. In general, this reactor type shows disadvantages in terms of heat management and resistance against carbon depositions on the catalyst. Especially, the heat evolution and therefore the temperature peaks in the adiabatic reactors necessitate a reactor cascade and increase the complexity of the process setup [11, 12]. Simultaneously to fixed beds, research activities concerning the development of fluidized beds as methanation reactors started [13]. One of the most prominent fluidized bed concepts is the COMFLUX process, which successfully demonstrated the production of 20 MW_{SNG} from coal. The 1 MW_{SNG} fluidized bed methanation unit connected to the DFB gasifier in Güssing on the other hand was developed by the Paul Scherrer Institut (PSI) and was the first demonstration of a biomass-to-SNG process on a large scale [10]. Fluidized beds can overcome the limitations imposed to fixed beds by their inherently good heat and mass transfer. This results in nearly isothermal operation conditions and an intrinsic catalyst regeneration [14]. However, high particle forces and therefore high attrition rates have prevented the commercialization of fluidized beds in catalytic methanation processes so far. Continued research work is thus put into the development of appropriate catalysts as reported in [15–17]. Other research groups focus on the development of structured reactors. The catalyst is dispersed on thermally highly conducting structures, thus reducing temperature hotspots. This concept, for example, was applied by the Engler-Bunte-Institut for the load-flexible methanation of gasifier product gas with additional hydrogen from electrolysis [12] or by Biegger et al. [18] for a power-to-gas (PtG) concept with a honeycomb methanation catalyst. The variety of reactor types also explains the wide range of operation conditions in the methanation reactor. Temperatures from 250 to 700 °C and pressures from 1 to 87 bar_a have been applied. From a thermodynamic point of view, the methanation is favored at low temperatures and high pressures. A more comprehensive comparison of different reactor concepts can be found in literature [10–13].

Depending on the composition of the raw-SNG after methanation, different gas upgrading steps might be necessary before the gas can be fed to the gas grid. In the case of DFB gasification and the consecutive catalytic methanation, the upgrading steps can include drying, CO_2 separation, and H_2 separation. Various kinds of CO_2 separation technologies have been proposed for this task. Heyne and Harvey [19] compared membranes, pressure swing adsorption (PSA), and chemical absorption with monoethanolamine and concluded that chemical absorption results in the highest cold gas efficiencies. Physical absorption is another method for the removal of CO_2. However, high pressures are usually required for these processes and Gassner and Maréchal [20] showed that it is the least favorable option for allothermal gasification processes compared with PSA and membrane technologies. For the separation of H_2, mainly membrane technologies are proposed [19–21]. However, to the best of our knowledge, no comparative study on H_2 separation technologies for the investigated process has been carried out so far.

In order to feed the generated gas into the Austrian gas grid, the feed-in regulations must be satisfied. In Austria, the limits for the most important accompanying substances are defined at 4 vol.-% for H_2 and 2 vol.-% for CO_2. Limitations for other trace substances and calorific properties are defined as well but are not relevant to this investigation. The values are standardized in [22, 23]. Interestingly, there is no specification mentioned for CO. This is due to the fact that the guidelines were developed for natural gas and later extended to biogas from biological methanation. Both sources do not contain CO and therefore this issue has not arisen. However, for the SNG production via the thermochemical pathway, a limit for the CO content would be necessary to ensure a high quality gas. This is an issue not only in Austria but also all around Europe, since no threshold levels are defined as summarized in [24]. Currently, the discussion focuses on an increased H_2 content in the natural gas grids all around Europe [25]. Studies have shown that up to 10 vol.-% of H_2 in the natural gas grid has no adverse effects on the grid and most applications [26, 27]. However, as long as this is not transferred to national or European law, the strict limits—as defined before—must be fulfilled. Therefore, an alternative is the generation of a CH_4/H_2 mixture, also referred to as hythane, which can be used as a substitute for natural gas directly in industrial applications without the need to feed it into the gas grid first [28].

In Güssing (Austria) and Gothenburg (Sweden), two plants for the conversion of woody biomass to SNG were operated on a large scale. Both concepts utilized a DFB gasification process but applied different gas cleaning and synthesis steps. In Gothenburg, an adapted four-step adiabatic fixed bed methanation process with intermediate cooling was used (TREMP process). Additionally, a water-gas shift reactor, a pre-methanation reactor, and an amine-based CO_2 separation

unit were installed upstream of the methanation reactors. The gasifier system was operated with a thermal fuel power of 32 MW_{th} and therefore was the largest DFB gasifier built so far. The DFB section was operated in total for 12,000 h with wood pellets and later with wood chips and forest residues as feedstock. During the operation, they identified some issues regarding the fuel feeding, the tar formation, and the product gas cooling [29]. Because of these problems, the SNG production periods were quite limited but nevertheless about 67 GWh of SNG was produced in total. From December 2017 to February 2018, they achieved the design goal and the installed capacity of 20 MW_{SNG} was reached. Chemical efficiencies for the production of SNG from 50 to 63% with wood pellets were reported. The carbon utilization efficiency was about 30%, which means that 30% of the carbon in the biomass is transferred to the SNG while the rest is exhausted mainly as CO_2 [30].

In contrast to this concept, the Güssing plant utilized a single fluidized bed methanation reactor and the amine-based CO_2 separation was performed downstream of the methanation reactor. Unlike the GoBiGas plant, a membrane for the separation of excess H_2 was required as the final gas-upgrading step. The 1 MW_{SNG} methanation section was mainly operated in 2009 and was the first plant to produce SNG from woody biomass on a demonstration scale. The gas was not injected into the gas grid but was stored in a compressed natural gas (CNG) tank. Nevertheless, the Austrian gas grid specifications were reached and SNG with about 95 vol.-% CH_4 and 3.8 vol.-% of N_2 in minor amounts of H_2, CO_2, CO, and C_2H_6 was produced. Additionally, a cold gas efficiency of 62% is reported for this process [31]. Because of the application of a fluidized bed methanation reactor the Güssing concept allowed a simpler process setup compared to GoBiGas. However, the Güssing setup was the first of its kind and was not optimized technically. The methanation section applied in Gothenburg on the other hand is commercially available and technically optimized to the specific requirements of the plant [10, 12].

Several other concepts follow the same goal to convert biogenic feedstock to SNG. Anaerobic digestion allows bacteria to convert non-woody biomass to biogas with approximately 60 vol.-% CH_4 and 40 vol.-% CO_2. This biogas can then be upgraded to SNG quality by removing the CO_2 and other minor impurities [32]. The same concept is applied to biogas from landfills or wastewater treatment plants where the biogas is produced naturally without the additional supply of feedstock [33].

Besides biological approaches, a significant amount of research is put into PtG concepts. The hydrogen produced via electrolysis can be utilized to methanate various kinds of carbon resources as the comprehensive review by Götz et al. [34]

shows. One of these sources is the separated CO_2 from biogas plants, which can be upgraded to CH_4 by catalytic methanation instead of the simple exhaustion. One of the most prominent representatives of this technology is the Audi e-gas plant in Germany, which uses a molten salt cooled tube bundle reactor [10]. Besides the classical PtG concepts, also hybrid processes have been developed. For example, Witte et al. [35] directly upgraded the biogas to biomethane on a smaller scale in Switzerland by feeding it together with hydrogen to a bubbling fluidized bed reactor. Instead of the downstream catalytic methanation, Bensmann et al. [36] on the other hand proposed a direct introduction of the hydrogen into the biogas reactor which induced a biological methanation process. Other hybrid concepts add hydrogen to the product gas of a biomass gasification process in order to increase the hydrogen to carbon ratio and therefore increase the overall carbon utilization efficiency of the biomass-to-SNG process. Here, the DemoSNG project is mentioned, where this combination was experimentally tested with a honeycomb-type methanation reactor. It was shown that despite the fluctuating availability of the hydrogen, a continuous production of SNG was possible [37].

From a thermodynamic point of view, the main chemical species which are involved in the methanation reaction system are CH_4, H_2, CO, CO_2, and H_2O. The corresponding reaction equations are the CO methanation (Eq. 1),

$$CO + 3H_2 \rightleftharpoons CH_4 + H_2O \qquad \Delta H_R^{300} = -216\frac{kJ}{mol} \qquad (1)$$

the reverse water-gas shift reaction (Eq. 2), and

$$CO_2 + H_2 \rightleftharpoons CO + H_2O \qquad \Delta H_R^{300} = 39\frac{kJ}{mol} \qquad (2)$$

the CO_2 methanation (Eq. 3) which is a combination of Eq. 1 and Eq. 2.

$$CO_2 + 4H_2 \rightleftharpoons CH_4 + 2H_2O \qquad \Delta H_R^{300} = -177\frac{kJ}{mol} \qquad (3)$$

Additionally, the reaction enthalpies at 300 °C (ΔH_R^{300}) are given. Besides these species, the product gas of the DFB gasifier also contains hydrocarbons. As one of the main components, ethylene (C_2H_4) is identified and is thus included here [38]. The hydrogenation to methane is given in Eq. 4.

$$C_2H_4 + 2H_2 \rightarrow 2CH_4 \qquad \Delta H_R^{300} = -209\frac{kJ}{mol} \qquad (4)$$

A deactivation mechanism of the catalyst, which cannot be prevented by gas cleaning steps, is the formation of solid carbon on the catalyst. While adsorbed carbon on the catalyst surface is a necessary reaction intermediate during

methanation, the formation of stable deposits leads to catalyst fouling [39]. Thermodynamically, this deposition can be accounted for by the Boudouard reaction in Eq. 5.

$$2CO \rightleftharpoons CO_2 + C(s) \qquad \Delta H_R^{300} = -174 \frac{kJ}{mol} \qquad (5)$$
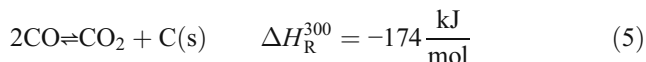
The deposited surface carbon can also be hydrogenated to methane according to Eq. 6,

$$C(s) + 2H_2 \rightleftharpoons CH_4 \qquad \Delta H_R^{300} = -82.1 \frac{kJ}{mol} \qquad (6)$$
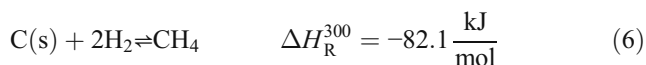
or undergo gasification with steam as shown in Eq. 7 [40].

$$C(s) + H_2O \rightleftharpoons CO + H_2 \qquad \Delta H_R^{300} = 134 \frac{kJ}{mol} \qquad (7)$$

These reactions show that increased amounts of H_2, H_2O, or CO_2 in the gasifier product gas might prevent the carbon deposition.

A different form of deposition occurs through the adsorption of hydrocarbons like C_2H_4 on the catalyst surface. Between 500 and 800 °C, the adsorption can lead to coke deposits [40]. In general, there is a large number of different forms and structural types of carbon or coke deposits which can occur at different temperature intervals in methanation processes [41].

If kinetic models are considered, all of the abovementioned reaction pathways have to be taken into consideration. The catalytic methanation of syngas is, however, mostly limited by heat transfer and not by kinetics under typical operating conditions. This limitation mostly applies for fixed bed reactors and thus multiple reactors with intermediate cooling are necessary in order to manage the heat released by the exothermic reactions [10]. Fluidized beds were shown to overcome this limitation and allow a low-temperature methanation in a single reactor step. The process was mainly found to be limited by the mass transfer between the bubble and the dense phase of the fluidized bed. Nevertheless, the gas composition is close to the thermodynamic equilibrium for temperatures down to 320 °C and kinetic limitations apply for lower temperatures as some studies confirm [17, 42, 43]. Additionally, the adjustment of the H_2/CO ratio of the feed gas to the required level of three can be directly carried out in the fluidized bed methanation reactor. Fixed bed applications usually require a separate water-gas shift reactor upstream of the methanation for this task [44, 45]. A thermodynamic calculation including the water-gas shift reaction thus provides a good estimation of the expected gas composition. Because of the broad variety of possible carbon species, deviations from the thermodynamic equilibrium for carbon depositions have to be expected [10]. Nevertheless, graphitic carbon has previously been used to elucidate this issue since kinetic models are often only valid for specific reaction conditions and catalysts [46].

Extensive studies have been performed on the thermodynamics of methanation. Bia et al. [39] used ternary diagrams to visualize the calculated boundaries of carbon formation under methanation conditions. Frick et al. [46] applied the same method but extended the investigation to different feed gas mixtures. They concluded that ternary diagrams are an appropriate tool for the design of methanation processes. Gao et al. [47] performed a systematic thermodynamic investigation on the methanation of CO and CO_2 under varying parameters like pressure, temperature, or the H_2/CO ratio. As a result, they give general indications on the effects of the parameter variations. Other research groups extended the modelling to a larger part of the process setup and used different modelling approaches. For example, Witte et al. [48] used rate-based modelling and investigated different combinations of methanation reactors and hydrogen membranes to upgrade biogas from biological digestion to biomethane. In order to upgrade the biogas, they proposed a PtG concept with renewable hydrogen via electrolysis. They concluded that, in order to reach the gas grid requirements, a combination of a bubbling fluidized bed reactor with a second-stage fixed bed methanation unit or a gas separation membrane are the technically and economically favorable options [49]. Neubert [50] proposed a similar two-stage methanation setup within the PtG concept. The first stage consists of a structured methanation reactor followed by an intermediate water condensation and a second-stage fixed bed reactor. Within his work, he elaborately used thermodynamic models and ternary diagrams to define the optimal CO_2 removal as well as steam and hydrogen addition in general. For the production of SNG from coal, Liu et al. [51] used thermodynamic calculations in Aspen Plus to find the most suitable process setup. They concluded that a circulating fluidized bed followed by a second-stage fixed bed methanation reactor poses the most promising concept. For small-scale air blown biomass gasifiers Vakalis et al. [52] thermodynamically modelled the methanation with additional hydrogen. They reached CH_4 concentrations of only 40 mol.-% because of the high N_2 concentrations inherent to the product gas of air-blown gasifiers. The modelling of a combination of the SER process with a TREMP methanation process was carried out in [53]. They reached cold gas efficiencies of 62% with this setup and about 60% when additional hydrogen from an electrolyzer was added. In [54], three different gasifier types were compared for the production of SNG with the conclusion that allothermal gasification systems, like the DFB system, result in the highest overall efficiencies. Rönsch et al. [11] give a comprehensive overview over many different modelling approaches for methanation reactors and SNG production plants. Depending on the scope of the study, the investigations range from detailed one-, two-, or three-dimensional methanation reactor models to flow sheet simulations of entire SNG process chains with zero-dimensional equilibrium models. However, no evaluation of

the results from the latest DFB gasifier design in terms of SNG production has been carried out. Furthermore, no detailed thermodynamic analysis of the SNG production from biogenic residues exists and no evaluation of the process in terms of the carbon utilization efficiency is reported.

In this paper, a thermodynamic model of a fluidized bed methanation reactor is developed and applied to specific feed gas mixtures, which have been obtained by experimental gasification test runs of different biogenic residues with a new generation of a 100 kW$_{th}$ DFB gasifier at TU Wien. The chosen feed gas compositions for the methanation aim at covering the broad range of product gas compositions which can be produced by the DFB gasifier. The results show a detailed thermodynamic analysis of the raw-SNG gas compositions and key values for different feed gas mixtures and varying operation conditions like temperature and pressure. These results are discussed and evaluated in terms of their suitability for a feed-in into the natural gas grid. Because of the different process setups regarding the CO_2 separation unit in Güssing and Gothenburg, the placement of the CO_2 separation unit upstream or downstream of the methanation reactor is discussed as well.

2 Concept and methodology

In order to calculate the thermodynamic equilibrium, only four of the seven reaction equations (Eq. 1 to Eq. 7) need to be considered. Otherwise, the system would be overdetermined, because only four equations are linearly independent of each other. For example, the CO_2 methanation reaction can be seen as the reversed water-gas shift reaction followed by the CO methanation.

Thermodynamic calculations were performed with HSC Chemistry 6 and MATLAB. HSC Chemistry is a commercially available software tool for thermodynamic calculations and contains a database with thermodynamic property data. It calculates the thermodynamic equilibrium concentrations with the Gibbs free energy minimization method. For the purpose of this work, a MATLAB-based program for the thermodynamic equilibrium calculations was developed. This program calculates the thermodynamic equilibrium based on the temperature dependent thermodynamic property data from HSC Chemistry. The solution was obtained by numerically solving the equilibrium constant expressions for each reaction equation. The equilibrium concentrations were then automatically plotted over temperature and pressure. The model was validated by comparing the calculated results on a random basis to results obtained with HSC Chemistry. This comparison showed that the model is highly accurate.

Figure 1 visualizes the modelling approach with a basic flowsheet. In the DFB gasification process, the feedstock is converted to the gasifier product gas. The validated results for a multitude of experimental test runs in a 100 kW$_{th}$ DFB gasifier at TU Wien have already been published elsewhere (see Sect. 3) and are used as a basis for the modelling of the methanation in this study. In the gas cleaning section, impurities like dust, tar, as well as sulfur and nitrogen containing contaminants are removed. The gas cleaning is not included in the model because it does not influence the thermodynamic calculations of the methanation. Therefore, the gas cleaning is treated as a black box which removes all impurities except ethylene. Ethylene was found to be the main hydrocarbon in the gasifier product gas besides CH_4 which is not removed by conventional gas cleaning steps like scrubbers or activated carbon filters. Besides ethylene, also hydrocarbons like benzene, toluene, xylene, or naphthalene are often not completely removed [55–57]. In this investigation, they are neglected because the concentrations are comparably low. After the gas cleaning, the gasifier product gas is fed to the methanation unit. Here, the thermodynamic model is applied and the conversion of the feed gas to raw-SNG is calculated. Since the raw-SNG does not fulfill the requirements of the gas grid, the necessary gas upgrading steps are also discussed but not modelled. Optionally, the CO_2 separation can be carried out as shown in Fig. 1 or as part of the raw-SNG upgrading after the methanation reactor. The standard setup in this investigation is the downstream CO_2 separation as part of the raw-SNG upgrading. However, also the upstream CO_2 separation as indicated in Fig. 1 is discussed.

The main focus of this investigation is a low-temperature methanation (300 °C) at ambient pressure. These parameter settings result from the current efforts on the scientific investigation of a novel bench-scale fluidized bed methanation setup for the given parameters. As the DFB gasification process also operates at ambient pressure an additional energy input for compression is avoided. This bench-scale methanation setup has been designed and built at TU Wien and is currently in the commissioning phase. Nevertheless, also a temperature variation from 200 to 500 °C and a pressure range from 1 to 10 bar$_a$ are investigated. While thermodynamic calculations are in general independent of the reactor design, the validity of the underlying assumptions is nevertheless defined by the process-related circumstances. In this study, this translates to the following assumptions: (i) the water-gas shift reaction takes place simultaneously to the methanation reactions in one reactor without a need for a prior adjustment of the H_2/CO ratio, (ii) C_2H_4 is hydrogenated to methane, and (iii) despite the high exothermicity of the reactions, a low-temperature methanation (e.g. 300 °C) is possible in one reactor. These assumptions are only valid for fluidized bed methanation but would not be valid for fixed bed methanation as reported in literature [10, 44, 45, 58]. Graphite is chosen as the prevailing carbon species, since Frick et al. [46] found that
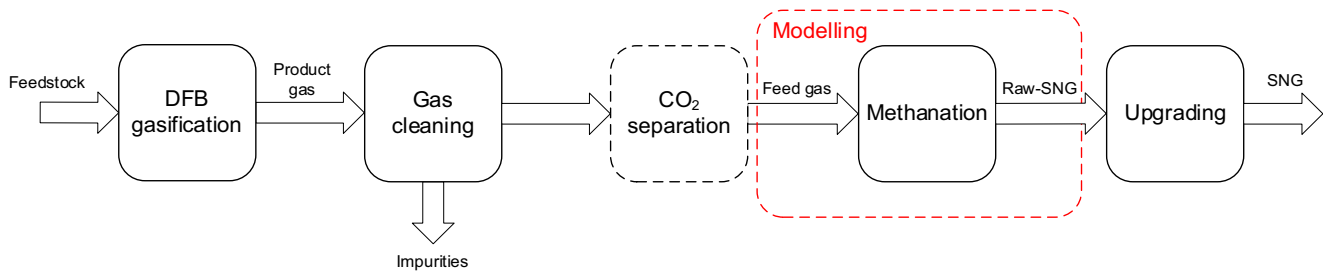
Fig. 1 SNG production flowsheet via the DFB gasification route; the highlighted area defines the modelled part of the process in this study

the Gibbs free energy is lower than for amorphous carbon and is thus preferentially formed.

In order to classify the feed gas composition, the stoichiometric number (SN) is defined in Eq. 8.

$$SN = \frac{y_{H_2}}{3\,y_{CO} + 4\,y_{CO_2} + 2\,y_{C_2H_4}} \qquad (8)$$

SN gives the ratio between the molar fraction of H_2 (y_{H_2}) to the molar fractions of the carbonaceous species in the feed gas which react to CH_4. If SN is equal to 1, there is a stoichiometric amount of H_2 available according to Eqs. 1, 3, and 4. Because the regarded pressures in this study are relatively low, an ideal gas behavior is assumed and molar fractions are thus equal to volume fractions. The definition of SN is not unambiguous, because the chemical equilibrium is influenced by all available species and therefore also by CH_4 and H_2O. Nevertheless, it allows an approximate classification of the feed gas mixture. Typical product gases from the DFB gasification of biogenic feedstock show similar CH_4 concentrations; moreover H_2O concentrations in the feed gases are assumed 0. The latter is attributed to the required gas cleaning which is conventionally carried out at low temperatures [59]. If similar CH_4 concentrations and a water-free feed gas are assumed, the implementation of SN is justified.

Additionally, the CH_4 yield (Y_{CH_4}) is defined in Eq. 9. It describes how much of the carbon in the feed gas is converted to CH_4.

$$Y_{CH_4} = \frac{\dot{n}_{CH_4,eq}}{\sum_i N_i\,\dot{n}_{i,feed}} \times 100 \qquad (9)$$

The carbon yield (Y_C) in Eq. 10 is a measure for carbon deposition.

$$Y_C = \frac{\dot{n}_{C,eq}}{\sum_i N_i\,\dot{n}_{i,feed}} \times 100 \qquad (10)$$

Index i refers to the carbonaceous species in the feed ($i = CH_4$, CO, CO_2, C_2H_4), and N_i is the number of carbon atoms in species i.

The CO conversion (X_{CO}) in Eq. 11 gives the amount of CO which is converted during the reaction.

$$X_{CO} = \frac{\dot{n}_{CO,feed} - \dot{n}_{CO,eq}}{\dot{n}_{CO,feed}} \times 100 \qquad (11)$$

Analogously to Eq. 11, the CO_2 conversion (X_{CO_2}) is defined in Eq. 12.

$$X_{CO_2} = \frac{\dot{n}_{CO_2,feed} - \dot{n}_{CO_2,eq}}{\dot{n}_{CO_2,feed}} \times 100 \qquad (12)$$

In order to assess the performance of the overall process, the carbon utilization efficiency (η_C) is introduced (Eq. 13). It sets the amount of carbon in the methane of the raw-SNG ($\dot{n}_{CH4,eq}$) in relation to the amount of carbon which is introduced to the process via the feedstock ($\dot{n}_{C,feedstock}$). If CO_2 is used as gasification agent, the amount of carbon in the gasification agent must be considered as well ($\dot{n}_{C,gasif}$). The carbon utilization efficiency illustrates how much of the carbon is valorized as CH_4 in the SNG and how much is "lost" mainly as CO_2.

$$\eta_C = \frac{\dot{n}_{CH4,eq}}{\dot{n}_{C,feedstock} + \dot{n}_{C,gasif}} = \eta_{C,DFB} \times Y_{CH4} \qquad (13)$$

An analogous way to calculate the carbon utilization efficiency is by the multiplication of the carbon utilization efficiency over the DFB gasifier ($\eta_{C,DFB}$) and the methane yield in the methanation section (Y_{CH4}). In this paper, $\eta_{C,DFB}$ is calculated from the validated results of test runs with the 100 kW_{th} DFB gasifier at TU Wien. This value is therefore only valid for this gasifier. An extrapolation of $\eta_{C,DFB}$ to large-scale gasifiers is not recommended since the internal energy and mass balances might differ. In this small-scale gasifier, the high heat losses are balanced by the addition of heating oil in the combustion section of the DFB process which is not the case for large-scale plants. Large-scale gasifiers exhibit much lower heat losses, but, depending on the feedstock, a partial recycling of product gas to the combustion section might still

be necessary. The recycled amount of product gas is not available for methanation. This factor cannot be considered in the calculation, and the shown results therefore need to be seen as a maximum.

Additionally, the minimum amount of steam (H_2O_{feed}), which needs to be added upstream of the methanation reactor to prevent carbon formation, is introduced. In order to calculate H_2O_{feed}, every investigated reaction condition with each feed gas is checked for the possibility of carbon formation. If carbon formation is possible, the water content in the feed gas is incrementally increased until the thermodynamic possibility for carbon formation yields 0. At this point, H_2O_{feed} can be obtained. Furthermore, gas cleaning is not within the scope of this study and the feed gas mixtures for the methanation are assumed free of impurities and other minor components. Besides, kinetics or heat and mass transfer phenomena are not considered.

3 Results and discussion

Table 1 shows the investigated feed gas compositions for the methanation derived from DFB gasification. In the upper part of the table, the operational parameters of the DFB gasification process are shown. All displayed feed gas compositions are obtained with a new generation 100 kW_{th} DFB gasifier at TU Wien. The DFB process is not elaborated in this study and further information can be found in literature [4, 7, 8, 56, 60, 61]. The lower part of Table 1 depicts the gas compositions which are derived from the DFB gasification process and are in further consequence used as the feed gas compositions for the methanation process. All feed gases are assumed to be free of

H_2O. Feed gas no. 1 shows a typical SER product gas with a high hydrogen content. Limestone (L) is used as bed material, and bark (BA) is chosen as feedstock. Feed gas no. 2–no. 4 present product gases from conventional gasification. With feed gas no. 2, the same fuel and bed material as with feed gas no. 1 is used but the gasification temperature is higher which results in lower H_2 and higher CO and CO_2 contents. For feed gas no. 3, lignin (LI) is used as fuel and olivine (O) as bed material. Sewage sludge (SS) and an olivine/limestone mixture (O/L) are the basis for feed gas no. 4, which results in low H_2 and high CO_2 contents. For feed gas no. 5, a CO_2/H_2O mixture is used as gasification agent and rapeseed cake (RSC) and O as fuel and bed material, respectively. This results in even lower H_2 and high CO and CO_2 concentrations. Feed gas no. 6 shows a temperature variation for SER gasification. This is included to demonstrate the adaptability of the DFB gasification process to the requirements of the methanation process (cf. Fig. 6). Data for this variation is only available for softwood (SW) as feedstock.

In Fig. 2, the results of the chemical equilibrium calculations at 300 °C and 1 bar_a are shown for feed gas nos. 1–5. The volume fractions of the dry gas components after the methanation (referred to as raw-SNG) and the water content of the raw-SNG ($H_2O_{raw-SNG}$) as well as the minimum required water content in the feed gas in order to prevent carbon deposition (H_2O_{feed}) are depicted.

Additionally, Table 2 lists some key figures as defined in Eqs. 8–12 complementary to the results in Fig. 2. In Fig. 2a and the left part of Table 2 (without H_2O_{feed}), the results for a water-free feed gas are displayed. Figure 2b and the right part of Table 2 (with H_2O_{feed}) display the results with steam addition to the feed gases in order to prevent carbon formation. C_2H_4 is not depicted in any of the figures, because it is

Table 1 Investigated feed gases

DFB parameters	Unit	Feed gas number					
		1	2	3	4	5	6
Source	–	[8]	[4]	[56]	[7]	[60]	[61]
Gasification agent	–	H_2O	H_2O	H_2O	H_2O	CO_2/H_2O[a]	H_2O
Feedstock	–	BA	BA	LI	SS	RSC	SW
Bed material	–	L	L	O	O/L[b]	O	L
Gasification temperature	°C	625	761	789	800	840	582–797
Combustion temperature	°C	820	998	945	945	938	830–1041
Feed gas composition to methanation (water-free feed)							
H_2	vol.-%	68.3	51.1	42.6	35.6	25.8	71.1–47.6
CO	vol.-%	6.5	17.9	21.2	13.7	32.1	7.3–21.6
CO_2	vol.-%	8.9	22.4	21.8	36.5	33.7	4.1–23
CH_4	vol.-%	14.5	8.0	12.0	11.7	7.3	17.4–8.8
C_2H_4	vol.-%	1.9	0.6	2.4	2.5	1.1	1.9–0.5

[a] CO_2/H_2O = 68/32 vol.-%

[b] O/L = 80/20 wt.-%
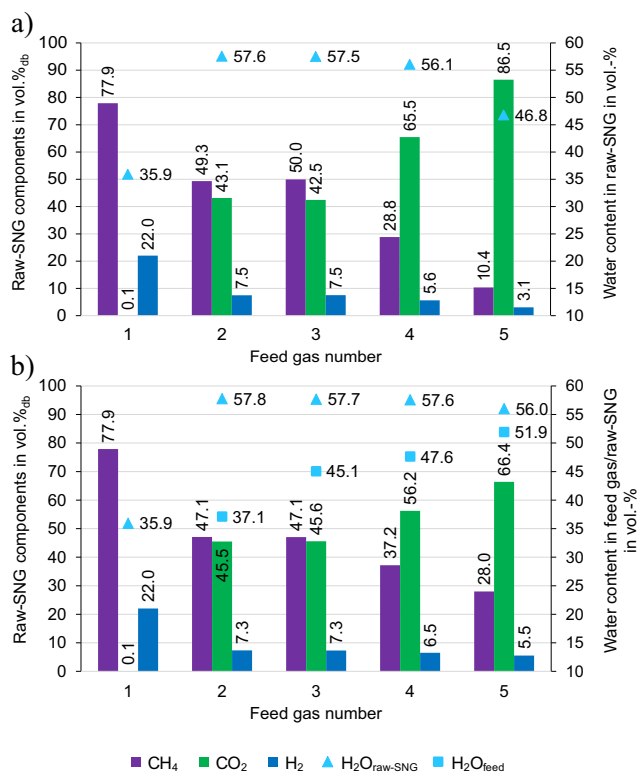
Fig. 2 Raw-SNG gas composition for feed gas nos. 1–5 at 1 bar$_a$ and 300 °C. **a** Water-free feed gas. **b** Feed gas with steam addition to prevent carbon deposition

completely converted under all investigated conditions. CO is also not shown in Fig. 2 because it is almost entirely converted (see Table 2) and only trace amounts remain in the raw-SNG. The feed gases are displayed in descending order for *SN* in Fig. 2 as well as in Table 2. This results in a decreasing trend for CH$_4$ and H$_2$ and an increasing trend for CO$_2$ in the raw-SNG. Analogously, the methane yield and the CO$_2$ conversion drop significantly with understoichiometric feed gases.

A closer look at the results for the water-free feed gases reveal that the SER feed gas (feed gas no. 1) allows an almost complete conversion of CO and CO$_2$ to CH$_4$. Thus, no CO$_2$ separation is necessary. In addition, no carbon formation is thermodynamically expected. However, 22 vol.-%$_{db}$ of H$_2$ is still in the raw-SNG and needs to be separated below 4 vol.-%

before grid feed-in according to the Austrian regulations [22, 23]. Feed gas nos. 2–5 result in a lower CH$_4$ content and a higher CO$_2$ content. The CO conversion is almost complete even though *SN* is well below one for feed gas nos. 2–5. This is possible because thermodynamically the feed-CO is rather converted to solid carbon than left unreacted in the raw-SNG. This results in severe carbon depositions with a carbon yield as high as 54.5%. More than half of the carbon in the feed would be deposited on the catalyst. This deposition would result in a high loss of carbon and deactivate the catalyst. Therefore, feed gas nos. 2–5 should not be introduced into the methanation reactor without a previous steam addition. Thus, in Fig. 2b and the right part of Table 2, the results with the addition of steam to the feed gas are depicted. The amount of steam added corresponds to the minimum amount needed to prevent carbon formation. For feed gas no. 1, no steam addition is necessary and therefore the results are the same as in Fig. 2a. All other feed gases require steam addition in a range of 37 to 52 vol.-%. The raw-SNG for these feed gases therefore shows a different composition compared with the water-free feed gases. For feed gas nos. 2 and 3, about half the raw-SNG consists of CH$_4$, the rest is CO$_2$ and H$_2$. For feed gas nos. 4 and 5, CO$_2$ constitutes the main component in the raw-SNG with a CH$_4$ yield of approximately 40% and 30%, respectively. All four gas compositions require the separation of both CO$_2$ and H$_2$ before grid feed-in, even if the less stringent limitation of 10 vol.-% H$_2$ is applied. Compared with the results of the dry feed gases, the CH$_4$ yield is slightly increased but the CO$_2$ conversion is significantly lowered. All four gases show a negative CO$_2$ conversion, which implies that more moles of CO$_2$ are produced than consumed during the reaction. The influence of the steam addition on the reactions can be pictured as follows: The water-gas shift reaction (Eq. 2) proceeds towards CO$_2$ and H$_2$. This way, more H$_2$ is available for the methanation of CO and less CO needs to be methanated because it is shifted towards CO$_2$. The additional H$_2$ is used to hydrogenate the solid carbon. From this point of view, it also becomes apparent that the CO$_2$ conversion is less compared with the results of the water-free feed or even negative. There are of course many ways to illustrate this effect. The reaction pathway is only important for the consideration

Table 2 Key figure results of the equilibrium calculations

| Parameter	Unit	Feed gas number (without H$_2$O$_{feed}$)					Feed gas number (with H$_2$O$_{feed}$)				
		1	2	3	4	5	1	2	3	4	5
SN	-	1.16	0.35	0.27	0.19	0.11	1.16	0.35	0.27	0.19	0.11
Y_{CH_4}	%	99.9	28.2	24.6	14.4	5.2	99.9	50.8	49.2	39.8	29.6
Y_C	%	0	47.2	54.5	52.8	50.9	0	0	0	0	0
X_{CO}	%	100	99.9	99.9	99.8	99.9	100	99.8	99.8	99.6	99.8
X_{CO_2}	%	99.7	45.6	42.7	39.9	2.2	99.7	−8.5	−34.9	−10.3	−57.1

of kinetic effects and does not influence the thermodynamic equilibrium. Table 2 shows that the CO conversion remains almost complete for all feed gases. Nevertheless, the CO_2 methanation is found to be kinetically inhibited even for very low CO concentrations [62]. For feed gas no. 1, only 7 $ppm_{v,db}$ of CO remain in the raw-SNG in the thermodynamic equilibrium. At least 600–700 $ppm_{v,db}$ need to be expected for feed gas nos. 2–5. As long as there are no regulations on the allowed CO content, no statement about the grid feed-in can be made. The authors recommend a threshold value for CO if the production of SNG via the thermochemical pathway is further pursued at industrial scale.

3.1 Investigation of the sewage sludge product gas

In the following section, a more in-depth discussion of the feed gas derived from SS gasification follows (feed gas no. 4). Because of the expected carbon deposition for this feed gas composition, H_2O should be added if a long catalyst lifetime and a high conversion efficiency are aimed at. This was already discussed in the previous section. Hence, Fig. 3 depicts the raw-SNG gas composition after the addition of steam for a temperature variation from 200 to 500 °C and pressures of 1, 5, and 10 bar_a (Fig. 3b). The amount of steam added corresponds to the minimum amount needed to prevent carbon

Fig. 3 Temperature and pressure variation for feed gas no. 4 in the thermodynamic equilibrium: 1 bar_a (full line), 5 bar_a (dashed line), and 10 bar_a (dash-dotted line). **a** CH_4 yield and feed water content. **b** Raw-SNG gas composition

deposition. This minimum volume fraction of H_2O in the feed gas (H_2O_{feed}) as well as Y_{CH_4} is also displayed (Fig. 3a). With increasing temperature, less CH_4 and CO_2 and more CO and H_2 are present. Accordingly, the CH_4 yield decreases from 41 to 26% with increasing temperature at 1 bar_a. H_2O_{feed} decreases from 55 to 40 vol.-% within the displayed temperature range. Nevertheless, the methanation is preferred at low temperatures from a thermodynamic point of view if the additionally required steam is not seen as the decisive factor. Especially, the low methane yield and the strongly rising CO content at higher temperatures make low-temperature methanation attractive. Pressure only has a significant influence on the gas composition at higher temperatures. At 500 °C, Y_{CH_4} can be substantially elevated and the H_2 content significantly lowered if the pressure is increased to 5 bar_a. A further pressurization only allows a minor improvement of Y_{CH_4} but still reduces the H_2 content by 5 percentage points. At 200 °C, Y_{CH_4} is almost constant for all pressures. For H_2O_{feed}, hardly any influence of pressure can be observed.

In general, this feed gas shows a rather unfavorable composition for methanation. The stoichiometric number is far below 1, and the CO_2 content in the feed gas is even higher than the H_2 content. For grid feed-in, the CO_2 needs to be separated from the raw-SNG. A maximum of only 2 vol.-% is allowed. A H_2 content below the allowed threshold level of 4 vol.-% after CO_2 separation and without an additional H_2 separation unit could be achieved by increasing the pressure at 260 °C to 5 bar_a or at 280 °C to 10 bar_a. If the stringent feed-in specification of the natural gas grid is loosened and 10 vol.-% H2 is allowed in the future, the methanation can be performed at 350 °C at 10 bara, 320 °C at 5 bara, or 270 °C at 1 bara. Even though there is only a slight influence of pressure on the gas composition at these temperatures, a small increase can nevertheless enable the grid feed-in without an H2 separation unit. This is especially interesting if 10 vol.-% of H2 would be allow in the gas grid because the reaction temperature would be in a range where catalysts were found to be kinetically active. If the desired commodity is hythane, only CO2 separation is necessary and the discussion concerning the H2 content and the pressurization can be neglected.
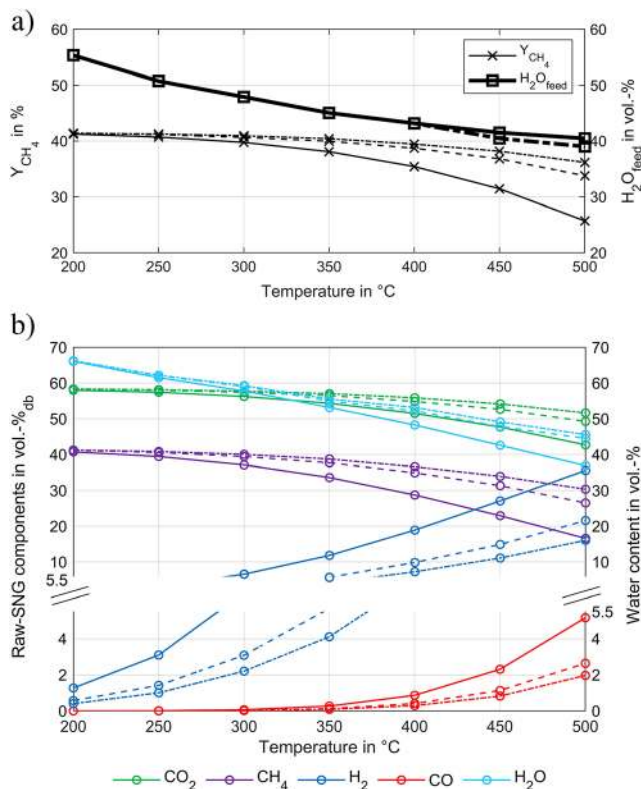
3.2 Investigation of the feed gases with upstream CO_2 separation

Firstly, the upstream CO_2 separation is discussed with the sewage sludge product gas (feed gas no. 4) in detail before the discussion is extended to all other investigated feed gas compositions. In Fig. 4, the equilibrium calculations for feed gas no. 4 in a temperature range from 200 to 500 °C and pressures of 1, 5, and 10 bar_a are shown. In contrast to Fig. 3, the CO_2 separation is done upstream of the methanation reactor as demonstrated in the GoBiGas project in
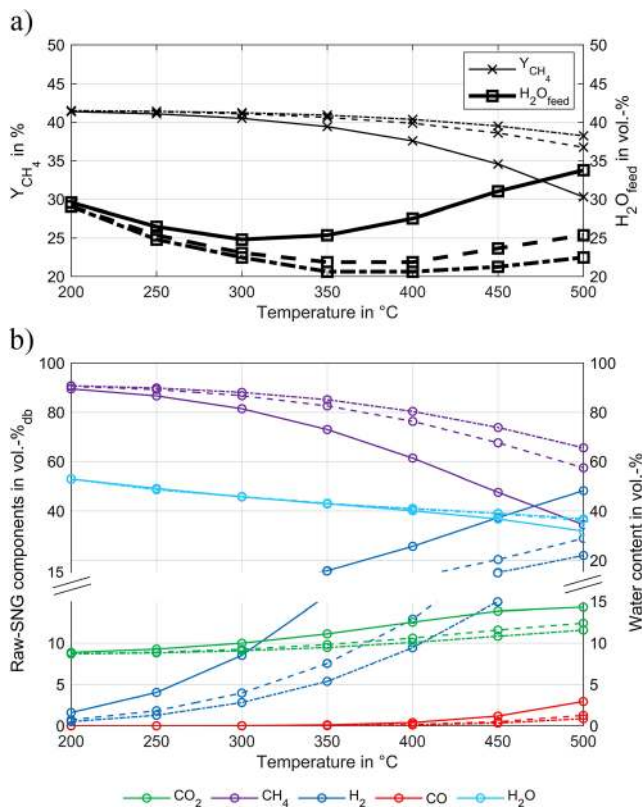
Fig. 4 Temperature and pressure variation for feed gas no. 4 in the thermodynamic equilibrium with CO_2 separation upstream of the methanation: 1 bar_a (full line), 5 bar_a (dashed line), and 10 bar_a (dash-dotted line). a CH_4 yield and feed water content. b Raw-SNG gas composition

Gothenburg. The feed gas to the methanation is therefore free of CO_2. In order to enable a fair comparison to Fig. 3, the calculation of the methane yield includes the CO_2 separation step in this case. A comparison between Figs. 3 and 4 reveals that Y_{CH_4} is slightly increased, whereas the required amount of steam in the feed is substantially lowered. The lower amount of steam in the feed could lead to a more energy-efficient process because less steam needs to be provided to the methanation reactor. Interestingly, at higher temperatures, H_2O_{feed} increases again and the pressure sensitivity is much more pronounced in comparison. The H_2 content is a little higher and the CO content slightly lower (e.g., 250 $ppm_{v,db}$ compared with 667 $ppm_{v,db}$ at 300 °C and 1 bar_a) comparing CO_2 separation upstream and downstream of the methanation reactor. The CO_2 content is in a range of 9 to 15 vol.-%$_{db}$, which implies that CO_2 is formed during the reaction. The CO_2 content as well as the higher H_2 and lower CO content in the raw-SNG can be explained by the water-gas shift reaction (Eq. 2) which is shifted towards CO_2 and H_2 due to the missing CO_2 and the understoichiometric H_2/CO ratio in the feed. In this case, the CO_2 needs to be separated again, which requires a second CO_2 separation unit. The same applies for feed gas nos. 2, 3, and 5. These feed gases also have a H_2/CO ratio

below 3, and therefore CO_2 is formed during the reaction in an order that it exceeds the limit of 2 vol.-% for all investigated operation conditions. Hence, a simple process setup with a single CO_2 separation step upstream of the methanation reactor does not suffice for a single stage methanation when understoichiometric feed gases, like feed gas nos. 2–5, are introduced to the methanation reactor. Two possible arrangement results are as follows: (i) The CO_2 separation unit is placed downstream of the methanation reactor. The resulting disadvantage is the slightly lower methane yield, as shown above, and a higher gas volume flow through the methanation reactor because of the surplus CO_2. The latter increases the capital expenditures (CAPEX) of the methanation reactor. On the other hand, the strong volume contraction during methanation reduces the gas flow through the CO_2 separation unit which in turn reduces the CAPEX. (ii) A CO_2 separation unit is placed upstream and downstream of the methanation reactor. The methane yield is slightly higher and the gas flow through the methanation is lower. The disadvantages in this case are the increased CAPEX for the second CO_2 separation step and the increased heat flux in the methanation reactor due to the missing ballast gas. Hence, the second option does not seem to be favorable because of the additionally required process unit in the case of a single stage fluidized bed methanation with the investigated understoichiometric feed gases (feed gas nos. 2–5). For the SER feed gases (feed gas no. 1 and no. 6), the CO_2 separation can be neglected completely if the right operating conditions are chosen as is explained below. For a multistage process, like GoBiGas, the upstream CO_2 removal is nevertheless justified. The water-gas shift reaction is carried out in a separate reactor followed by the CO_2 separation unit, both upstream of the methanation reactors. This way, the production of CO_2 and surplus H_2 in the methanation section can be suppressed and no further gas upgrading besides drying is necessary.

3.3 Investigation of the SER product gas

Feed gas no. 1 is a typical SER product gas with a high H_2 content. The SN is greater than 1, which allows a practically complete methanation of the carbonaceous species (CO + CO_2 + C_2H_4) at temperatures up to 300 °C with a CH_4 yield of nearly 100% (Fig. 5).

Pressure only has a significant influence on the gas composition at higher temperatures. With pressurization, the decreasing trend of CH_4 and the increasing trends of H_2, CO, and CO_2 at higher temperatures can be counteracted. In addition, above 440 °C at 1 bar_a carbon formation is thermodynamically possible. As is shown in Fig. 5a, H_2O needs to be added in this small operating window. At higher pressures, the steam addition can be prevented. Below 300 °C, there is practically no influence of pressure or temperature on the gas composition. In this case, methanation around 300 °C and
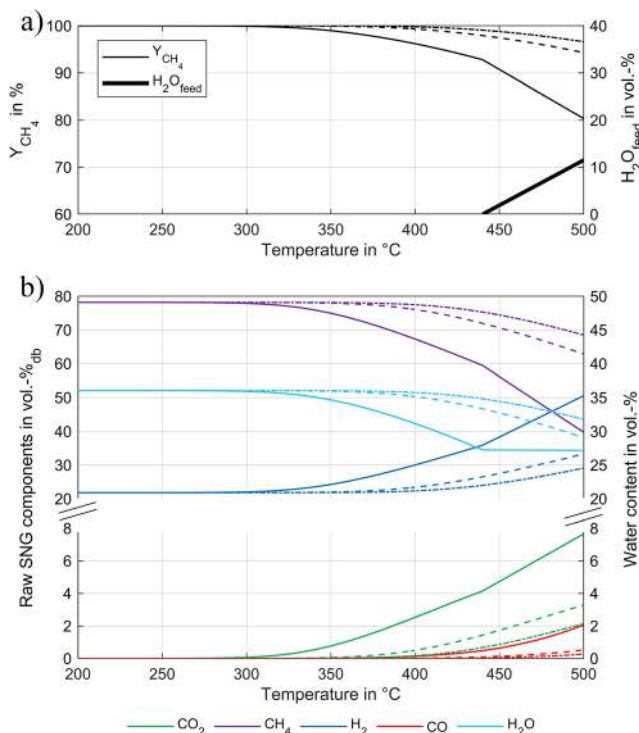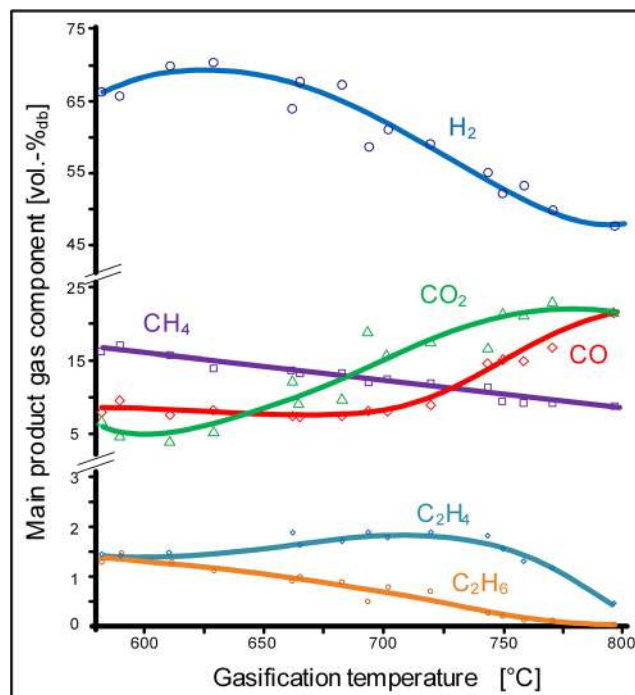
Fig. 5 Temperature and pressure variation for feed gas no. 1 in the thermodynamic equilibrium: 1 bar$_a$ (full line), 5 bar$_a$ (dashed line), and 10 bar$_a$ (dash-dotted line). **a** CH$_4$ yield and feed water content. **b** Raw-SNG gas composition

Fig. 6 Product gas composition over gasification temperature for the 100 kW$_{th}$ DFB gasifier at TU Wien for softwood and olivine as fuel and bed material, respectively (from [61])

1 bar$_a$ shows a favorable raw-SNG composition without the need of compression. Lower temperatures would not improve the gas composition but increase the challenge of employing an active catalyst. For grid feed-in, only H$_2$ would need to be separated from the raw-SNG. For the application as hythane on the other hand, no further upgrading step is necessary except water condensation.

3.4 Investigation of variable product gas compositions of the SER process

Fuchs et al. [61] already described the adaptability of the SER process with regard to the product gas composition. In Fig. 6, the evolution of the product gas components over the gasification temperature of the 100 kW$_{th}$ DFB gasifier at TU Wien is depicted. The product gas can be adjusted to the required feed gas for methanation by varying the gasification temperature. However, this also adds an additional parameter to the modelling of the methanation reactions. The range for the gas components, the temperatures, the used bed material, and the fuel is already listed in Table 1 (feed gas no. 6).

Figure 7 displays the composition of the raw-SNG in the thermodynamic equilibrium for all data points of Fig. 6 over SN. Temperature and pressure are again set to 300 °C and 1 bar$_a$ respectively, for the methanation process. In order to assess the carbon formation, Y_C is given. There is a decreasing

trend for CO$_2$, H$_2$O, and the amount of carbon formed for an increasing SN. CH$_4$ has a maximum at a SN slightly above 1. At the same point, carbon formation declines to 0 and the small incline in H$_2$ turns into a sharp increase for higher SN. CO is only present in trace amounts (0.14–614 ppm$_{v,db}$) and is not displayed here. From a thermodynamic point of view, the feed gas with a SN of 1.09 results in a raw-SNG with the most favorable composition for the methanation at 300 °C and 1 bar$_a$. A SN of 1.09 corresponds to a gasification temperature of about 680 °C. The associated compositions for the feed gas and the raw-SNG as well as the key figures are depicted in Table 3. Both CO and CO$_2$ are almost completely converted and therefore no CO$_2$ separation step is necessary. Compared with feed gas no. 1 the H$_2$ content is lower but for grid feed-in the H$_2$ still needs to be separated. A pressure increase to 4 bar$_a$ lowers the H$_2$ content below 10 vol.-%, and the raw-SNG could be directly utilized as SNG without further purification if the loosened H$_2$ restriction in the gas grid is assumed. This would be an economic improvement because no H$_2$ separation step is necessary. Additionally, the CH$_4$ yield and the CO$_2$ conversion increase and the CO content decreases. The according raw-SNG composition and the key figures at 4 bar$_a$ and 300 °C are also displayed in Table 3. Different operation conditions of the methanation might favor other feed gas compositions from Fig. 6 and vice versa. In order to find the most suitable feed gas composition for deviating methanation conditions, reiterations of the thermodynamic equilibrium calculations would have to be carried out.

Fig. 7 Raw-SNG gas composition and Y_C over *SN* at 300 °C and 1 bar$_a$ for the feed gas compositions according to Fig. 6 in the thermodynamic equilibrium
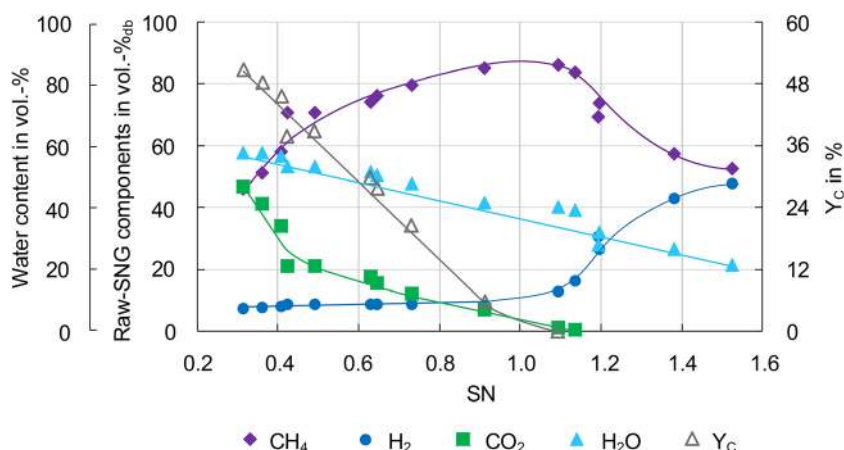
3.5 Comparison of all investigated feed gases with the carbon utilization efficiency

Table 4 compares the investigated feed gases (feed gas nos. 1–6) by means of the carbon utilization efficiencies (η_C, $\eta_{C,DFB}$) as well as the H_2 and CO_2 contents in the raw-SNG at 300 °C and 1 bar$_a$. η_C is the highest for the product gas from the gasification of LI (feed gas no. 3) and the lowest for the product gas from the CO_2 gasification of RSC (feed gas no. 5). All other values for η_C are in a similar range between 34.6 and 37.9%. The comparison of η_C and $\eta_{C,DFB}$ reveals that the carbon utilization for the SER product gases (feed gas no. 1 and 6) is governed by the carbon utilization in the DFB system. The excess carbon (in the form of CO_2), which is still in the raw-SNG in case of conventional gasification (like feed gas nos. 2–4), is already removed within the SER process by the increased transport of carbon from the fuel to the flue gas. This results in a low $\eta_{C,DFB}$ but a similar value for η_C compared with feed gas nos. 2 and 4 because nearly a complete carbon utilization is achieved in the methanation section. Additionally, no CO_2 separation step is required as the

possibility to adjust the stoichiometric number *SN* is inherent to the process. Further savings result from the fact that no steam addition to the feed gas is necessary and the fact that the composition of the feed gas can be adjusted (cf. Fig. 6). Despite the high flexibility, a H_2 separation is nevertheless required under current regulations. If 10 vol.-% of H_2 would be allowed, the SER process seems economically advantageous because neither a CO_2 nor a H_2 separation unit or a steam addition to the feed gas is required under the right process conditions (e.g. feed gas no. 6 at 300 °C and 4 bar$_a$). The CO_2 separation alone was estimated to account for 13–22% of the total fixed capital investment costs of a biomass-to-SNG plant [19].

The highest η_C is reached with feed gas no. 3, which originates from the gasification of lignin with olivine as bed material. The high η_C results from the high value for $\eta_{C,DFB}$. Almost 93% of the carbon in the fuel is relocated to the gasifier product gas. The lowest η_C results from feed gas no. 5, which originates from the gasification of rapeseed cake with olivine as bed material and a CO_2/H_2O mixture as gasification agent. The gasification with a CO_2 admixture to the

Table 3 Feed gas and raw-SNG composition and key figures for the feed gas with a *SN* of 1.09 at 300 °C and 1 bar$_a$ as well as 300 °C and 4 bar$_a$ in the thermodynamic equilibrium

Parameter	Unit	Feed gas	Raw-SNG at 1 bar$_a$	Raw-SNG at 4 bar$_a$
CH_4	vol.-%$_{db}$	13.3	86.1	90.0
H_2	vol.-%$_{db}$	67.8	12.8	9.8
CO	vol.-%$_{db}$	7.3	0.005	0.0008
CO_2	vol.-%$_{db}$	9.8	1.1	0.2
C_2H_4	vol.-%$_{db}$	1.7	0	0
H_2O	vol.-%	0	40.2	41.6
Y_{CH_4}	%	-	98.8	99.7
Y_C	%	-	0	0
X_{CO}	%	-	100	100
X_{CO_2}	%	-	95.8	99.1

Table 4 Comparison of the carbon utilization efficiencies and the H_2 and CO_2 contents in the raw-SNG for feed gas nos. 1–6 at 300 °C and 1 bar$_a$

Parameter	Unit	Feed gas number					
		1	2	3	4	5	6
$\eta_{C, DFB}$	%	36.5	72.8	92.6	86.9	78.0	38.4
η_C	%	36.5	37.0	47.0	34.6	23.1	37.9
H_2 content	vol.-%$_{db}$	22.0	7.3	7.3	6.5	5.5	12.8
CO_2 content	vol.-%$_{db}$	0.1	45.5	45.6	56.2	66.4	1.1

gasification agent therefore cannot be used advantageously for the production of SNG if no external hydrogen is provided. For feed gas nos. 2–5, a CO_2 separation and a H_2 separation is required. If the 10 vol.-% H_2 threshold is applied, the H_2 separation can be avoided (e.g. feed gas no. 4 at 320 °C and 5 bar$_a$). Even the 4 vol.-% H_2 threshold can be met if the operation conditions are adapted (e.g. feed gas no. 4 at 280 °C and 10 bar$_a$), but kinetic effects at these low temperatures most likely need to be considered. For these feed gases (feed gas nos. 2–5), the carbon utilization efficiency can be increased by the addition of H_2 from external sources (e.g. electrolysis) which allows the methanation of the leftover CO_2. From a technical and ecological point of view, the addition is advantageous since η_C can be maximized. The availability and the expenditures for the additional hydrogen on the other hand need to be eyed critically. In this paper, this concept is not discussed any further but some relevant studies were already referred above [50, 52].

In general, the calculated results are in good agreement with literature values. The GoBiGas plant reached a η_C of about 30%, which is slightly lower as most of the calculated values. The slightly lower values seem justified, since this study is based on thermodynamic calculations and therefore the results need to be seen as maximum values. The gasification section of the GoBiGas plant reached a $\eta_{C,DFB}$ of about 70% as can be calculated from the results in [63]. This value is similar to feed gas no. 2 but lower compared with all other feed gases. The discrepancy possibly arises from the small scale and good performance of the pilot plant as well as the difficult scalability of the carbon utilization efficiency as explained in the methodology section. Taking the results from the modelling study of Heyne and Harvey [19], a η_C of 35% can be calculated, which is very close to the calculated values in this paper. Also, the raw-SNG composition with 45 vol.-%$_{db}$ of CH_4, 47 vol.-%$_{db}$ of CO_2, and 4 vol.-%$_{db}$ of H_2 is close to the calculated values. Similar values were also reported by Gassner et al. [64] who calculated a raw-SNG composition with 45 vol.-%$_{db}$ CH_4, 45 vol.-%$_{db}$ CO_2, and 6 vol.-%$_{db}$ H_2. Both studies assumed similar operating conditions at approximately 300 °C and 1 bar$_a$. Experimentally, Seemann et al.

[58] confirmed a similar raw-SNG composition. They reconstructed the feed gas composition of the Güssing gasifier and reached slightly lower CH_4 concentrations at approximately 40 vol.-%$_{db}$ CH_4, 47 vol.-%$_{db}$ CO_2, and 4 vol.-%$_{db}$ H_2. The 1 MW$_{SNG}$ methanation plant in Güssing, however, could not meet the 4 vol.-% threshold, and a two-stage membrane separation process was necessary, whereas in Gothenburg, no H_2 separation unit was required [10, 31].

4 Conclusion and outlook

In this work, the suitability of various product gases from the 100 kW$_{th}$ DFB gasifier for methanation in a fluidized bed reactor was evaluated from a thermodynamic point of view. It was shown that a complete methanation of CO and CO_2 is only possible for SER product gases. For all other presented product gases, only the methanation of CO is possible, whereas CO_2 might even constitute the main raw-SNG component. Additionally, gases from conventional steam gasification or gasification with CO_2 admixture to the gasification agent ($H_2O + CO_2$) are subject to carbon depositions in the methanation reactor. Therefore, up to 55 vol.-% of H_2O needs to be added to the feed gas for a stable operation. Furthermore, the influence of different operation conditions of the methanation on the raw-SNG composition was visualized. By the careful choice of operation conditions, energy savings and/or less effort for further gas upgrading can be accomplished. A comparison between upstream and downstream CO_2 separation revealed that only a downstream CO_2 separation results in the required SNG quality if a single fluidized bed methanation reactor with understoichiometric feed gases is utilized. A further investigation of the SER product gases revealed that it is also possible to adapt the gasification process to suit certain methanation conditions. A SER product gas with a stoichiometric number of 1.09, which corresponds to a gasification temperature of 680 °C, was shown to be the most suitable feed gas for methanation. No CO_2 separation step and no H_2O addition to the feed gas was necessary, which clearly indicated an economic advantage. However, under current regulations, a H_2 separation unit could not be avoided for the raw-SNG from the SER product gas. An increase of the allowed H_2 content in the natural gas grid to 10 vol.-% would therefore increase the degrees of freedom of the whole system. In turn, this would result in improved operating points, which would simplify the overall process and reduce costs. This would apply for all investigated feed gases, but especially the SER process would benefit from these loosened restrictions. For example, the SER product gas (feed gas no. 6) could be methanated at 300 °C and 4 bar$_a$ to gas grid quality without a CO_2 or H_2 separation step nor a H_2O addition to the feed gas.

A comparison of the carbon utilization efficiencies revealed that the gasification of lignin resulted in the highest

overall value of 47%. Apart from one exception, all other values including the SER product gases range between 34.6 and 37.9%. Only if CO_2 is added to the gasification agent, the carbon utilization factor drops to 23%. The addition of H_2 from an external source would allow a much more efficient conversion of the carbon, but the availability and the economic implications would need to be considered.

It should be noted that all investigations in this paper are based on thermodynamic equilibrium calculations. Catalyst poisoning due to insufficient gas cleaning, kinetic limitations concerning carbon deposition, methanation of CO_2, the high feed water content, or low temperatures as well as possible heat or mass transfer limitations necessitate experimental investigations. These issues are subject of further investigations with the bench-scale fluidized bed methanation setup at TU Wien.

Abbreviations *BA*, bark; *bar$_a$*, bar absolute; *C*, carbon; *CNG*, compressed natural gas; *db*, dry basis; *DFB*, dual fluidized bed; *eq*, equilibrium; *feed*, in the feed gas; *gasif*, in the gasification agent; ΔH_R^{300}, molar reaction enthalpy at 300 °C; H_2O_{feed}, volume fraction of H_2O in the feed in vol.-%; *L*, limestone; *LI*, lignin; *O*, olivine; N_i, number of carbon atoms in species i; $\dot{n}_i$, molar flow of species i in mol/s; η_C, overall carbon utilization efficiency; $\eta_{C,\ DFB}$, carbon utilization efficiency over the DFB gasifier; *O/L*, olivine/limestone mixture; *PSA*, pressure swing adsorption; *PSI*, Paul Scherrer Institute; *PtG*, power-to-gas; *raw-SNG*, raw synthetic natural gas after methanation/before gas upgrading; *RSC*, rapeseed cake; *SER*, sorption enhanced reforming; *SN*, stoichiometric number; *SNG*, synthetic natural gas; *SS*, sewage sludge; *SW*, softwood; *v*, volumetric; *vol.-%*, volumetric percent; *wt.-%*, weight percent; X_{CO}, carbon monoxide conversion in %; X_{CO_2}, carbon dioxide conversion in %; Y_C, carbon yield in %; Y_{CH_4}, methane yield in %; y_i, molar fraction of species i

References

1. European Commission (2018) Directive (EU) 2018/2001 of the European Parliament and of the Council of 11 December 2018 on the promotion of the use of energy from renewable sources. Off J Eur Union L 328/82:128

2. International Energy Agency (2018) Gas 2018: analysis and forecasts to 2023. IEA. https://www.iea.org/reports/gas-2018. Accessed 29 March 2020

3. Wilk V (2013) Extending the range of feedstock of the dual fluidized bed gasification process towards residues and waste. Dissertation, TU Wien

4. Benedikt F, Schmid JC, Fuchs J, Mauerhofer AM, Müller S, Hofbauer H et al (2018) Fuel flexible gasification with an advanced 100 kW dual fluidized bed steam gasification pilot plant. Energy 164:329–343. https://doi.org/10.1016/j.energy.2018.08.146

5. Schweitzer D, Gredinger A, Schmid M, Waizmann G, Beirow M, Spörl R, Scheffknecht G (2018) Steam gasification of wood pellets, sewage sludge and manure: gasification performance and concentration of impurities. Biomass Bioenergy 111:308–319. https://doi.org/10.1016/j.biombioe.2017.02.002

6. Schmid JC, Wolfesberger U, Koppatz S, Pfeifer C, Hofbauer H (2012) Variation of feedstock in a dual fluidized bed steam gasifier-influence on product gas, tar content, and composition. Environ Prog Sustain Energy 31(2):205–215. https://doi.org/10.1002/ep.11607

7. Schmid JC, Bartik A, Benedikt F, Mauerhofer AM, Fuchs J, Schanz E, Reisinger S, Nowak B, Bühler F, Müller S, Fuchs M, Hofbauer H (2019) Steam gasification of sewage sludge for synthesis processes. In: Hofbauer H (ed) Proceedings of the ICPS 19, Vienna, pp 45-53

8. Fuchs J, Schmid JC, Müller S, Hofbauer H (2019) Dual fluidized bed gasification of biomass with selective carbon dioxide removal and limestone as bed material: a review. Renew Sust Energ Rev 107:212–231. https://doi.org/10.1016/j.rser.2019.03.013

9. Asadullah M (2014) Biomass gasification gas cleaning for downstream applications: a comparative critical review 40:118–132. https://doi.org/10.1016/j.rser.2014.07.132

10. Schildhauer TJ, Biollaz SMA (2016) Synthetic natural gas from coal, dry biomass, and power-to-gas applications. John Wiley & Sons, Hoboken

11. Rönsch S, Schneider J, Matthischke S, Schlüter M, Götz M, Lefebvre J, Prabhakaran P, Bajohr S (2016) Review on methanation – from fundamentals to current projects. Fuel 166:276–296. https://doi.org/10.1016/j.fuel.2015.10.111

12. Schildhauer TJ, Biollaz SMA (2015) Reactors for catalytic methanation in the conversion of biomass to synthetic natural gas (SNG). Chimia 69(10):603–607. https://doi.org/10.2533/chimia.2015.603

13. Kopyscinski J, Schildhauer TJ, Biollaz SMA (2010) Production of synthetic natural gas (SNG) from coal and dry biomass - a technology review from 1950 to 2009. Fuel 89(8):1763–1783. https://doi.org/10.1016/j.fuel.2010.01.027

14. Seemann MC, Schildhauer TJ, Biollaz SMA, Stucki S, Wokaun A (2006) The regenerative effect of catalyst fluidization under methanation conditions. Appl Catal A Gen 313(1):14–21. https://doi.org/10.1016/j.apcata.2006.06.048

15. Liu B, Ji S (2013) Comparative study of fluidized-bed and fixed-bed reactor for syngas methanation over Ni-W/TiO2-SiO2 catalyst. J Energy Chem 22(5):740–746. https://doi.org/10.1016/S2095-4956(13)60098-4

16. Liu J, Shen W, Cui D, Yu J, Su F, Xu G (2013) Syngas methanation for substitute natural gas over Ni–Mg/Al2O3 catalyst in fixed and fluidized bed reactors. Catal Commun 38:35–39. https://doi.org/10.1016/j.catcom.2013.04.014

17. Li J, Zhou L, Li P, Zhu Q, Gao J, Gu F, Su F (2013) Enhanced fluidized bed methanation over a Ni/Al2O3 catalyst for production of synthetic natural gas. Chem Eng J 219:183–189. https://doi.org/10.1016/j.cej.2013.01.005

18. Biegger P, Kirchbacher F, Medved A, Miltner M, Lehner M, Harasek M (2018) Development of honeycomb methanation catalyst and its application in power to gas systems. Energies 11(7): 1679. https://doi.org/10.3390/en11071679

19. Heyne S, Harvey S (2014) Impact of choice of CO_2 separation technology on thermo-economic performance of Bio-SNG production processes. Int J Energy Res 38(3):299–318. https://doi.org/10.1002/er.3038

20. Gassner M, Maréchal F (2012) Thermo-economic optimisation of the polygeneration of synthetic natural gas (SNG), power and heat from lignocellulosic biomass by gasification and methanation. Energy Environ Sci 5(2):5768. https://doi.org/10.1039/c1ee02867g

21. Rönsch S, Kaltschmitt M (2012) Bio-SNG production — concepts and their assessment. Biomass Conv Biorefin 2(4):285–296. https://doi.org/10.1007/s13399-012-0048-0

22. Österreichische Vereinigung für das Gas- und Wasserfach (2001) Richtlinie G 31: 2001-05 Erdgas in Österreich-Gasbeschaffenheit. ÖVGW. Accessed 29 March 2020

23. Österreichische Vereinigung für das Gas- und Wasserfach (2011) Richtlinie G B220: 2011-11 Regeneratives Gase – Biogas. ÖVGW. Accessed 29 March 2020

24. Thema M, Weidlich T, Hörl M, Bellack A, Mörs F, Hackl F, Kohlmayer M, Gleich J, Stabenau C, Trabold T, Neubert M, Ortloff F, Brotsack R, Schmack D, Huber H, Hafenbradl D, Karl J, Sterner M (2019) Biological CO_2-methanation: an approach to standardization. Energies 12(9):1670. https://doi.org/10.3390/en12091670

25. European Committee for Standardization (2018) Gas infrastructure-quality of gas-group H German Version (EN 16726:2015+A1: 2018)

26. European Commitee for Standardization (2016) Natural gas and biomethane for use in transport and biomethane for injection in the natural gas network - part 1: specifications for biomethane for injection in the natural gas network German Version (EN 16723–1: 2016)

27. Judd R, Pinchbeck D (2016) Hydrogen admixture to the natural gas grid. Compend Hydrog Energy 4:165–192. https://doi.org/10.1016/B978-1-78242-364-5.00008-7

28. Kraussler M, Schindler P, Hofbauer H (2017) An experimental approach aiming the production of a gas mixture composed of hydrogen and methane from biomass as natural gas substitute in industrial applications. Bioresour Technol 237:39–46. https://doi.org/10.1016/j.biortech.2017.03.040

29. Thunman H, Seemann M, Berdugo Vilches T, Maric J, Pallares D, Ström H, Berndes G, Knutsson P, Larsson A, Breitholtz C, Santos O (2018) Advanced biofuel production via gasification - lessons learned from 200 man-years of research activity with Chalmers' research gasifier and the GoBiGas demonstration plant. Energy Sci Eng 6(1):6–34. https://doi.org/10.1002/ese3.188

30. Larsson A, Gunnarsson I, Tengberg F (2018) The GoBiGas Project. Demonstration of the production of biomethane from biomass via gasification. Technical Report

31. Rehling B (2012) Development of the 1 MW Bio-SNG plant, evaluation on technological and economical aspects and upscaling considerations. Dissertation, TU Wien

32. Molino A, Nanna F, Ding Y, Bikson B, Braccio G (2013) Biomethane production by anaerobic digestion of organic waste. Fuel 103:1003–1009. https://doi.org/10.1016/j.fuel.2012.07.070

33. Rasi S (2009) Biogas composition and upgrading to biomethane. Dissertation, University of Jyväskyla

34. Götz M, Lefebvre J, Mörs F, McDaniel Koch A, Graf F, Bajohr S, Reimert R, Kolb T (2016) Renewable power-to-gas: a technological and economic review. Renew Energy 85:1371–1390. https://doi.org/10.1016/j.renene.2015.07.066

35. Witte J, Calbry-Muzyka A, Wieseler T, Hottinger P, Biollaz SMA, Schildhauer TJ (2019) Demonstrating direct methanation of real biogas in a fluidised bed reactor. Appl Energy 240:359–371. https://doi.org/10.1016/j.apenergy.2019.01.230

36. Bensmann A, Hanke-Rauschenbach R, Heyer R, Kohrs F, Benndorf D, Reichl U, Sundmacher K (2014) Biological methanation of hydrogen within biogas plants: a model-based feasibility study. Appl Energy 134:413–425. https://doi.org/10.1016/j.apenergy.2014.08.047

37. Bajohr S, Schollenberger D, Buchholz D, Weinfurtner T, Götz M (2014) Kopplung der PtG-Technologie mit thermochemischer Biomassevergasung: Das KIC-Projekt "DemoSNG". gwf - Gas|Erdgas (155): 470–475

38. Benedikt F, Kuba M, Christian J, Müller S, Hofbauer H (2019) Assessment of correlations between tar and product gas composition in dual fluidized bed steam gasification for online tar prediction. Appl Energy 238:1138–1149. https://doi.org/10.1016/j.apenergy.2019.01.181

39. Bai X, Wang S, Sun T, Wang S (2014) Influence of operating conditions on carbon deposition over a Ni catalyst for the production of synthetic natural gas (SNG) from coal. Catal Lett 144:2157–2166. https://doi.org/10.1007/s10562-014-1379-1

40. Kambolis A, Schildhauer TJ, Kröcher O (2015) CO methanation for synthetic natural gas production. Chimia 69(10):608–613. https://doi.org/10.2533/chimia.2015.608

41. Bartholomew CH (2001) Mechanisms of catalyst deactivation. Appl Catal A Gen 212(1–2):17–60. https://doi.org/10.1016/S0926-860X(00)00843-7

42. Kopyscinski J, Schildhauer TJ, Biollaz SMA (2011) Methanation in a fluidized bed reactor with high initial CO partial pressure : part I — experimental investigation of hydrodynamics, mass transfer effects, and carbon deposition. Chem Eng Sci 66(5):924–934. https://doi.org/10.1016/j.ces.2010.11.042

43. Kopyscinski J, Schildhauer TJ, Biollaz SMA (2009) Employing catalyst fluidization to enable carbon management in the synthetic natural gas production from biomass. Chem Eng Technol 32(3): 343–347. https://doi.org/10.1002/ceat.200800413

44. Lommerzheim W, Flockenhaus C (1978) One stage combined shift-conversion and partial methanation process for upgrading synthesis gas to pipeline quality. In: American Gas Association (ed) Proceedings of the Tenth Synthetic Pipeline Gas Symposium, Chicago, pp 439–451

45. Seemann M (2007) Methanation of biosyngas in a fluidized bed reactor: development of a one-step synthesis process, featuring simultaneous methanation, watergas shift and low temperature tar reforming. Dissertation, ETH Zurich

46. Frick V, Brellochs J, Specht M (2014) Application of ternary diagrams in the design of methanation systems. Fuel Process Technol 118:156–160. https://doi.org/10.1016/j.fuproc.2013.08.022

47. Gao J, Wang Y, Ping Y, Hu D, Xu G, Su F (2012) A thermodynamic analysis of methanation reactions of carbon oxides for the production of synthetic natural gas. RSC Adv 2:2358–2368. https://doi.org/10.1039/c2ra00632d

48. Witte J, Settino J, Biollaz SMA, Schildhauer T (2018) Direct catalytic methanation of biogas – part I: new insights into biomethane production using rate-based modelling and detailed process analysis. Energy Convers Manag 171:750–768. https://doi.org/10.1016/j.enconman.2018.05.056

49. Witte J, Kunz A, Biollaz SMA, Schildhauer T (2018) Direct catalytic methanation of biogas – part II: techno-economic process assessment and feasibility reflections. Energy Convers Manag 178: 26–43. https://doi.org/10.1016/j.enconman.2018.09.079

50. Neubert M (2019) Catalytic methanation for small- and mid-scale SNG production. Dissertation, Friedrich-Alexander-Universität

51. Liu J, Cui D, Yao C, Yu J, Su F, Xu G (2016) Syngas methanation in fluidized bed for an advanced two-stage process of SNG production. Fuel Process Technol 141:130–137. https://doi.org/10.1016/j.fuproc.2015.03.016

52. Vakalis S, Malamis D, Moustakas K (2018) Thermodynamic modelling of an onsite methanation reactor for upgrading producer gas from commercial small scale biomass gasifiers. J Environ

Manag 216:145–152. https://doi.org/10.1016/j.jenvman.2017.06.044

53. Martínez I, Romano MC (2016) Flexible sorption enhanced gasification (SEG) of biomass for the production of synthetic natural gas (SNG) and liquid biofuels: process assessment of stand-alone and power-to-gas plant schemes for SNG production. Energy 113:615–630. https://doi.org/10.1016/j.energy.2016.07.026

54. van der Meijden CM, Veringa HJ, Rabou LPLM (2010) The production of synthetic natural gas (SNG): a comparison of three wood gasification systems for energy balance and overall efficiency. Biomass Bioenergy 34(3):302–311. https://doi.org/10.1016/j.biombioe.2009.11.001

55. Nakamura S, Kitano S, Yoshikawa K (2016) Biomass gasification process with the tar removal technologies utilizing bio-oil scrubber and char bed. Appl Energy 170:186–192. https://doi.org/10.1016/j.apenergy.2016.02.113

56. Schmid JC, Benedikt F, Fuchs J, Mauerhofer AM, Müller S, Hofbauer H (2019) Syngas for biorefineries from thermochemical gasification of lignocellulosic fuels and residues - 5 years' experience with an advanced dual fluidized bed gasifier design. Biomass Convers Biorefin (2019). https://doi.org/10.1007/s13399-019-00486-2

57. Loipersböck J, Lenzi M, Rauch R, Hofbauer H (2017) Hydrogen production from biomass: the behavior of impurities over a CO shift unit and a biodiesel scrubber used as a gas treatment stage. Korean J Chem Eng 34(8):2198–2203. https://doi.org/10.1007/s11814-017-0130-1

58. Seemann MC, Schildhauer TJ, Biollaz SMA (2010) Fluidized bed methanation of wood-derived producer gas for the production of synthetic natural gas. Ind Eng Chem Res 49(15):7034–7038. https://doi.org/10.1021/ie100510m

59. Abdoulmoumine N, Adhikari S, Kulkarni A, Chattanathan S (2015) A review on biomass gasification syngas cleanup. Appl Energy 155:294–307. https://doi.org/10.1016/j.apenergy.2015.05.095

60. Mauerhofer AM, Müller S, Benedikt F, Fuchs J, Bartik A, Hofbauer H (2019) CO_2 gasification of biogenic fuels in a dual fluidized bed reactor system. Biomass Convers Biorefin. https://doi.org/10.1007/s13399-019-00493-3

61. Fuchs J, Schmid JC, Müller S, Mauerhofer AM, Benedikt F, Hofbauer H (2019) The impact of gasification temperature on the process characteristics of sorption enhanced reforming of biomass. Biomass Convers Biorefin. https://doi.org/10.1007/s13399-019-00439-9

62. Van Herwijnen T, Van Doesburg H., De Jong W.A. (1973) Kinetics of the methanation of CO and CO_2 on a nickel catalyst. J Catal 28(3):391–402. https://doi.org/10.1016/0021-9517(73)90132-2

63. Karlbrink M (2015) An evaluation of the performance of the GoBiGas gasification process. Master Thesis, Chalmers University of Technology

64. Gassner M, Baciocchi R, Maréchal F, Mazzotti M (2009) Integrated design of a gas separation system for the upgrade of crude SNG with membranes. Chem Eng Process Process Intensif 48(9):1391–1404. https://doi.org/10.1016/j.cep.2009.07.002